Developing Models for future Real-Time Platforms

Virtual Simulation and Design of New Components and Systems for Aircraft and Remotely Piloted Aircraft Systems

García-Hernández, L.[1]*; Cuerno-Rejado, C.; Gandía-Agüero, F.; Rodríguez-Sevillano, A.A.; Cerveró, A.; Moreno, G.; Barcala-Montejano, M.A.;*
Escuela Técnica Superior de Ingeniería Aeronáutica y del Espacio (ETSIAE)
Universidad Politécnica de Madrid (UPM)
Madrid, Spain

Peña-Rodríguez, A.; Estensoro-Astigarraga, F.J.; Lasa-Aguirrebengoa, J.; Pelayo-Rivera, A.;
Tecnalia Research & Innovation,
Parque Tecnológico Zamudio 202
País Vasco, Spain

***Abstract*— In the development of electrified and other vehicle systems, the modelling and simulation of the vehicle is very important. With these tools the preliminary design, as well as later detailed studies of the systems developed, allow engineers to spend less time on each phase of their projects or address them with an integrated approach. In addition, this integrated approach provides the possibility of building hardware-in-the-loop models with all the components required. This vehicle modelling and simulation has gained more interest with the increasing use of a wide variety of RPAS, ranging from light weight micro aircraft to large vehicles of various tons. For this reason, the previously-described building tools are the final objective of the developing models to be used in real-time platform projects. The first step presented in this paper is to build a simulator that reproduces the behaviour of a selected aircraft and validate it. This paper presents the study of the performances and behaviour of an OPV used to validate the simulator developed later. At the end, some preliminary tests and estimations of the performances for the selected OPV with an electric motor are presented.**

Keywords—Software-in-the-loop; simulator; electric engine; hinge moment; actuator; hybridization; OPV; RPAS; design; components; emissions; HEV;

I. INTRODUCTION

The importance of emissions in aviation is a fact to be taken into account. The fuel consumed by U.S. commercial air carriers and the military releases more than 250 million tons of carbon dioxide (CO2) into the atmosphere each year. Other major emissions are NOx, SO2 and particulates. In addition, passenger air traffic is continuing to grow all around the world. However, there are research and innovation programmes aimed at reducing the emissions due to aircraft engines, like Horizon 2020. Also, great efforts have been made to develop green aviation in recent years [1]. Nowadays, research goals regarding the reduction of emissions are being established, and the progressive electrification of aircraft will probably be a part of the solution.

In line with what was mentioned in the previous paragraph, one solution is to use HEV (Hybrid Electrical Powertrains) instead of conventional powertrains, based on internal combustion engines burning fossil fuels. The possible configurations in HEVs are so different that aspects like energy efficiency, emissions, vehicle performance, range, etc., vary significantly. As all possible configurations have an electrical drive system, prior issues depend on the degree of hybridization and the control strategy employed. There are various key factors in the design stage of the electrical powertrain, such as energy storage (batteries, super-capacitors, etc.), electric machines, power inverters, etc., so the know-how is really important. All these components and many others are complex and require the use of advanced tools to perform the modelling and simulation in the conceptual and preliminary designs. After the powertrain architecture is defined, in the detailed design stage, model-based studies are required in order to implement control and optimization strategies for the management of the different energy sources. Based on all the foregoing, Tecnalia has developed Dynacar as a tool for the previously-mentioned purposes of developing road vehicles [2], [3]. The project described in this paper is similar to Dynacar, but in an aeronautical context.

In conclusion, the development of modelling and simulation tools has aroused great interest due to the increasing use of RPAS (Remotely Piloted Aircraft Systems), especially for new emerging commercial uses. In fact, this has driven the development of new design processes with all the components present to ensure the precision and requirements of the different possible systems, from the beginning stages of the process to the final adjustments. Also, the HEV as a part of the RPAS is of great interest for reducing local emissions and engine noise, especially in urban zones where the pollution is higher.

In this work, an OPV has been used (Optionally Piloted Vehicle). This type of aircraft can be piloted on board or remotely. That is why an OPV can be deployed in segregated and non-segregated airspace. In addition, it has high reliability and lower direct operating costs than RPAS. These features give the OPV an advantage over RPAS in equipment testing. In accordance with the above-mentioned, it would seem interesting to build and develop tools based on Hardware-in-the-Loop and Human-in-the-Loop using an OPV. This solution means that equipment can be developed which can be later

1. Corresponding author e-mail: luis.garcia.hernandez@alumnos.upm.es

incorporated into RPAS, while keeping a low design cost and ensuring a safe integration into aircraft architecture.

II. P2006T AIRCRAFT

The OPV chosen for the project was the P2006T airplane. This aircraft has some desirable features for carrying out SAR (Search and Rescue) missions. For example, a high wing that enables the Earth's surface to be observed from the cockpit without any obstacles. INDRA has worked with the P2006T platform and has equipped it to accomplish different missions related to maritime surveillance, intelligence and reconnaissance. The platform developed has been named as the P2006T MRI Surveillance System [4].

A. Features of the P2006T

The most important features and performances of the P2006T are shown below.

1) Main weights:

- MTOW (*Maximum Take-Off Weight*): 1230 kg.
- OEW (*Operating Empty Weight*): 760 kg.
- MPL (*Maximum Payload*): 380 kg.
- MFW (*Maximum Fuel Weight*): 144 kg.

2) Rotax 912 S3 engine main characteristics:

- Max. power and rotational speed at take-off: 73.5 kW at 5800 RPM.
- Max. continuous power and rotational speed: 69 kW at 5500 RPM.

3) Performances:

- Max. level speed at S/L: 287 km/h.
- Cruising speed at 65% power and 7000 ft.: 250 km/h.
- Range at 65% power with 30 minute reserves: 1148 km.
- Service ceiling: 4572 m.

These data will be contrasted later with the output data from the simulator developed throughout the present work in order to study the precision of the results.

B. Design mission

To compute the parameters for modelling the behaviour of the P2006T a design mission needs to be defined. This mission has been determined using INDRA´s scenarios to operate the aircraft and its studies on the camera equipped in the P2006T. According to this, the design mission will be defined by an altitude, a speed and a weight. The values of these parameters are:

- Altitude: 2134 m.
- Speed: 250 km/h (at 7000 ft. and 65% power).
- Weight: 1148 kg.

Secondly, the altitude profile for the design mission was designed. This profile consists of different stages: take-off, climb and cruise until the P2006T reaches the exploration zone, descent to the design altitude, recognition cruise with another descent to an identification altitude, a climb again to the recognition altitude, and at the end of the mission, a climb to a cruise altitude to return to base, the final descent and landing.

Figure 1 shows one possible INDRA scenario, the altitudes profile of the design mission and the detection and recognition capability of the camera at the design altitude.

III. BUILDING THE ORIGINAL SIMULATOR

First, an investigation of the different available flight simulators was carried out and afterwards FlightGear was selected as the graphical interface and connected with Simulink to build the simulator. Simulink allows programming whatever is needed in order to improve accuracy. Also the model can be modified and new modules, etc. can be implemented.

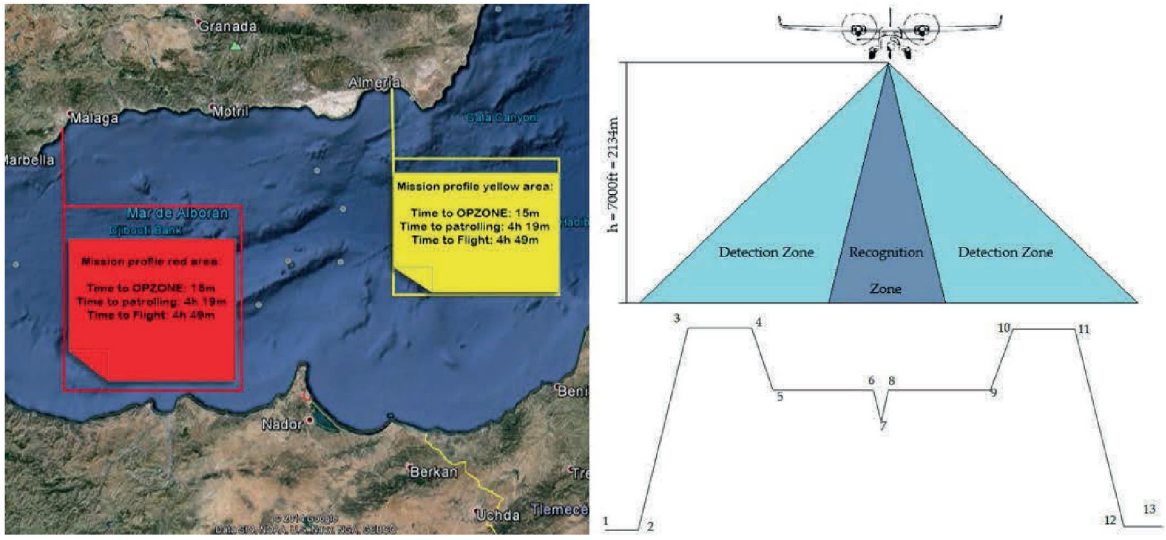

Fig. 1. Design mission for the P2006T. [15], [16], [17]

To solve the flight dynamic equations it is necessary to calculate the aerodynamic forces and moments. These forces and moments are obtained with the stability derivatives. Digital DATCOM stability derivatives [5] was developed and also a Roskam procedure [6], [7] to estimate the same coefficients that result from DATCOM. Then, both coefficients were compared to ensure the exactitude of the simulations.

The input archive of the Digital DATCOM provides the stability derivatives according to the geometry represented in Figure 2, which is compared with the actual geometry of the P2006T.

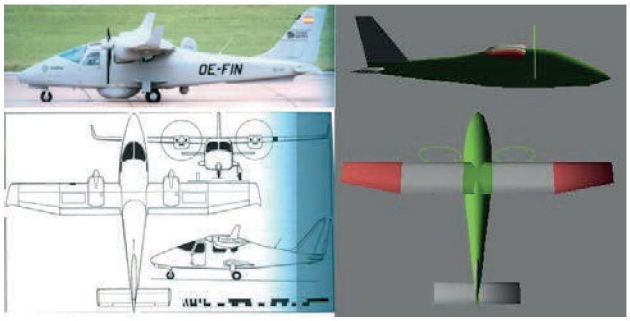

Fig. 2. Different view of the actual P2006T [12] and DATCOM output.

A part of the results obtained using DATCOM can be seen in Figure 3. Using these data it is possible to calculate the aerodynamic forces and moments that affect the aircraft in every flight condition, except for stall condition. The aerodynamic forces and moments are [8]:

$$\Delta X = X_u \Delta u + X_w \Delta w + X_{i_h} \Delta i_h \quad (1)$$

$$\Delta Y = Y_v \Delta v + Y_p \Delta p + Y_r \Delta r + Y_{\delta_r} \Delta \delta_r \quad (2)$$

$$\Delta Z = Z_u \Delta u + Z_w \Delta w + Z_q \Delta q + Z_{\dot{w}} \Delta \dot{w} + Z_{i_h} \Delta i_h \quad (3)$$

$$\Delta L = L_v \Delta v + L_p \Delta p + L_r \Delta r + L_{\delta_a} \Delta \delta_a + L_{\delta_r} \Delta \delta_r \quad (4)$$

$$\Delta M = M_u \Delta u + M_w \Delta w + M_q \Delta q + M_{\dot{w}} \Delta \dot{w} + M_{i_h} \Delta i_h \quad (5)$$

$$\Delta N = N_v \Delta v + N_p \Delta p + N_r \Delta r + N_{\delta_a} \Delta \delta_a + N_{\delta_r} \Delta \delta_r \quad (6)$$

The flight reference condition in stability axes is defined as [8]:

$$v_1 = \beta_1 = 0 \quad (7)$$

$$\phi_1 = 0 \quad (8)$$

$$p_1 = q_1 = r_1 = \dot{\psi}_1 = \theta_1 = \dot{\phi}_1 = 0 \quad (9)$$

$$\alpha_1 = w_1 = 0 \quad (10)$$

Using the flight dynamic equations at the reference condition, denoted with subscript 1, introducing a perturbation in the state variables, linearizing the equations ignoring the second order terms due to the perturbation, and eliminating the reference condition, leads to the set of dimensional equations:

$$-mg \cos\theta_1 \, \Delta\theta + \Delta X = m\Delta\dot{u} \quad (11)$$

$$mg \cos\theta_1 \, \Delta\phi + \Delta Y = m(\Delta\dot{v} + u_1 \Delta r) \quad (12)$$

$$-mg \sin\theta_1 \, \Delta\theta + \Delta Z = m(\Delta\dot{w} - u_1 \Delta q) \quad (13)$$

$$\Delta L = I_x \Delta\dot{p} - J_{xz} \Delta\dot{r} \quad (14)$$

$$\Delta M = I_y \Delta\dot{q} \quad (15)$$

$$\Delta N = -J_{xz} \Delta\dot{p} + I_z \Delta\dot{r} \quad (16)$$

Making use of (1), (2), (3), (4), (5) and (6) the equations for the longitudinal problem are [8]:

$$\left(X_u - m\frac{d}{dt}\right)\Delta u + X_w \Delta w - mg \cos\theta_1 \, \Delta\theta = -X_{i_h} \Delta i_h \quad (17)$$

$$Z_u \Delta u + \left(Z_w + \left(Z_{\frac{dw}{dt}} - m\right)\frac{d}{dt}\right)\Delta w + \left[\left(Z_q + mu_1\right)\frac{d}{dt} - mg \sin\theta_1\right]\Delta\theta = -Z_{i_h}\Delta i_h \quad (18)$$

$$M_u \Delta u + \left(M_w + M_{\frac{dw}{dt}}\frac{d}{dt}\right)\Delta w + \left(M_q \frac{d}{dt} - I_y \frac{d^2}{dt^2}\right)\Delta\theta = -M_{i_h}\Delta i_h \quad (19)$$

While the dimensional equations for the lateral-directional problem are [8]:

$$\left(Y_v - m\frac{d}{dt}\right)\Delta v + Y_p \Delta p + (Y_r - mu_1)\Delta r + mg \cos\theta_1 \, \Delta\phi = -Y_{\delta_r}\Delta\delta_r \quad (20)$$

$$L_v \Delta v + \left(L_p - I_x \frac{d}{dt}\right)\Delta p + \left(L_r + J_{xz}\frac{d}{dt}\right)\Delta r = -L_{\delta_a}\Delta\delta_a - L_{\delta_r}\Delta\delta_r \quad (21)$$

$$N_v \Delta v + \left(N_p + J_{xz}\frac{d}{dt}\right)\Delta p + \left(N_r - I_z \frac{d}{dt}\right)\Delta r = -N_{\delta_a}\Delta\delta_a - N_{\delta_r}\Delta\delta_r \quad (22)$$

1
1 AUTOMATED STABILITY AND CONTROL METHODS PER APRIL 1976 VERSION OF DATCOM
CHARACTERISTICS AT ANGLE OF ATTACK AND IN SIDESLIP
WING-BODY-VERTICAL TAIL-HORIZONTAL TAIL CONFIGURATION
PROPELLER POWER EFFECTS INCLUDED IN THE LONGITUDINAL STABILITY RESULTS
TOTAL: TOTAL: P2006T Aircraft (Simple)

MACH NUMBER	ALTITUDE M	VELOCITY M/SEC	PRESSURE N/ M**2	TEMPERATURE DEG K	REYNOLDS NUMBER 1/ M	REF. AREA M**2	REFERENCE LENGTH LONG. M	LAT. M	MOMENT REF. CENTER HORIZ M	VERT M
0 .200	2000.00	66.50	7.9501E+04	275.154	3.8607E+06	14.760	1.340	11.200	5.250	.000

0 -----DERIVATIVE (PER RADIAN)-----

0 ALPHA	CD	CL	CM	CN	CA	XCP	CLA	CMA	CYB	CNB	CLB
-10.0	.041	-.605	.2836	-.603	-.065	-.470	5.969E+00	-6.762E-01	-5.712E-01	6.066E-02	-7.605E-02
-8.0	.032	-.407	.2662	-.407	-.025	-.653	5.683E+00	-8.011E-01			-7.807E-02
-6.0	.026	-.211	.2352	-.215	.003	-1.105	5.601E+00	-1.225E+00			-7.988E-02
-4.0	.023	-.019	.1905	-.021	.021	-9.177	5.616E+00	-1.455E+00			-8.145E-02
-2.0	.023	.177	.1445	.176	.029	.819	5.784E+00	-1.508E+00			-8.306E-02
-1.0	.025	.278	.1205	.278	.029	.434	5.900E+00	-1.553E+00			-8.391E-02
.0	.027	.381	.0955	.381	.027	.250	6.002E+00	-1.571E+00			-8.479E-02
1.0	.030	.486	.0707	.487	.022	.145	6.083E+00	-1.585E+00			-8.569E-02
2.0	.035	.592	.0452	.593	.014	.076	6.159E+00	-1.623E+00			-8.662E-02
5.0	.046	.699	.0190	.701	.003	.027	6.220E+00	-1.658E+00			-8.760E-02
4.0	.047	.808	-.0079	.809	-.010	-.010	6.284E+00	-1.711E+00			-8.862E-02
6.0	.063	1.028	-.0652	1.029	-.045	-.063	6.409E+00	-1.912E+00			-9.077E-02
8.0	.083	1.252	-.1313	1.251	-.092	-.105	5.923E+00	-2.187E+00			-9.302E-02
10.0	.104	1.438	-.2066	1.434	-.147	-.144	5.001E+00	-2.472E+00			-9.431E-02
12.0	.126	1.597	-.2907	1.588	-.209	-.183	4.235E+00	-2.753E+00			-9.490E-02

0	ALPHA	Q/QINF	EPSLON	D(EPSLON)/D(ALPHA)
	-10.0	.917	-2.277	.440
	-8.0	.969	-1.397	.439
	-6.0	1.000	-.519	.429
	-4.0	1.000	.319	.420
	-2.0	1.000	1.162	.424
	-1.0	1.000	1.586	.423
	.0	1.000	2.009	.426
	1.0	1.000	2.438	.428
	2.0	1.000	2.865	.427
	3.0	1.000	3.291	.425
	4.0	1.000	3.714	.420
	6.0	1.000	4.540	.395
	8.0	1.000	5.294	.345
	10.0	1.000	5.921	.275
	12.0	1.000	6.393	.230

1 AUTOMATED STABILITY AND CONTROL METHODS PER APRIL 1976 VERSION OF DATCOM
DYNAMIC DERIVATIVES
WING-BODY-VERTICAL TAIL-HORIZONTAL TAIL CONFIGURATION
TOTAL: TOTAL: P2006T Aircraft (Simple)

MACH NUMBER	ALTITUDE M	VELOCITY M/SEC	PRESSURE N/ M**2	TEMPERATURE DEG K	REYNOLDS NUMBER 1/ M	REF. AREA M**2	REFERENCE LENGTH LONG. M	LAT. M	MOMENT REF. CENTER HORIZ M	VERT M
0 .200	2000.00	66.50	7.9501E+04	275.154	3.8607E+06	14.760	1.340	11.200	3.250	.000

0 DYNAMIC DERIVATIVES (PER RADIAN)

0	-------PITCHING-------		-----ACCELERATION-----		------------ROLLING------------		---------YAWING---------		
0 ALPHA	CLQ	CMQ	CLAD	CMAD	CLP	CYP	CNP	CNR	CLR
-10.00	8.377E+00	-2.005E+01	2.445E+00	-8.571E+00	-5.653E-01	-4.113E-02	4.983E-02	-8.637E-02	-7.229E-02
-8.00			2.582E+00	-9.050E+00	-5.439E-01	-4.287E-02	3.332E-02	-8.700E-02	-3.474E-02
-6.00			2.600E+00	-9.115E+00	-5.227E-01	-4.419E-02	1.708E-02	-8.811E-02	1.243E-03
-4.00			2.549E+00	-8.935E+00	-5.205E-01	-4.513E-02	1.091E-03	-8.963E-02	3.564E-02
-2.00			2.568E+00	-9.002E+00	-5.415E-01	-4.628E-02	-1.531E-02	-9.154E-02	7.127E-02
-1.00			2.567E+00	-8.999E+00	-5.531E-01	-4.697E-02	-2.366E-02	-9.267E-02	8.975E-02
.00			2.581E+00	-9.047E+00	-5.636E-01	-4.773E-02	-3.209E-02	-9.392E-02	1.086E-01
1.00			2.597E+00	-9.103E+00	-5.729E-01	-4.859E-02	-4.061E-02	-9.530E-02	1.279E-01
2.00			2.588E+00	-9.070E+00	-5.812E-01	-4.944E-02	-4.922E-02	-9.682E-02	1.474E-01
3.00			2.574E+00	-9.023E+00	-5.883E-01	-5.037E-02	-5.791E-02	-9.849E-02	1.672E-01
4.00			2.545E+00	-8.919E+00	-5.941E-01	-5.135E-02	-6.670E-02	-1.003E-01	1.872E-01
6.00			2.394E+00	-8.393E+00	-5.980E-01	-5.346E-02	-8.476E-02	-1.044E-01	2.276E-01
8.00			2.093E+00	-7.338E+00	-5.274E-01	-5.617E-02	-1.068E-01	-1.090E-01	2.678E-01
10.00			1.666E+00	-5.841E+00	-4.143E-01	-5.714E-02	-1.282E-01	-1.128E-01	2.977E-01
12.00			1.433E+00	-5.021E+00	-3.273E-01	-5.601E-02	-1.448E-01	-1.161E-01	3.210E-01

Fig. 3. Digital DATCOM output.

The eigenvalues of the longitudinal problem can be calculated with (17), (18) and (19). In the same way, the eigenvalues of the lateral-directional problem can be calculated with (20), (21) and (22). The eigenvalues calculated for both problems are presented in Figure 4. These eigenvalues are used to calculate the eigenvectors of the P2006T to check the stability and the behaviour of the aircraft.

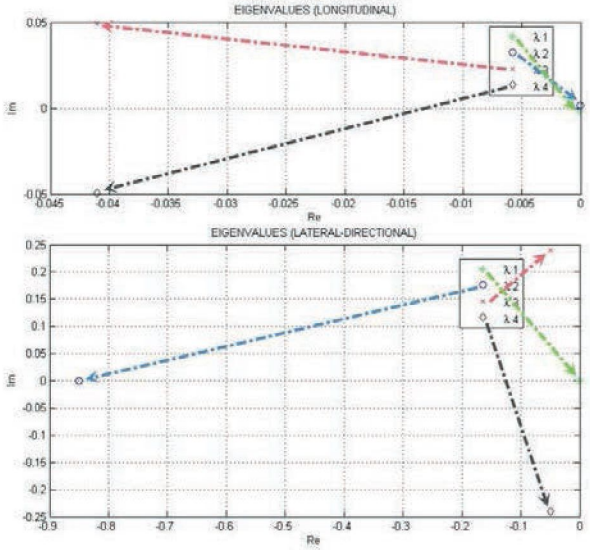

Fig. 4. Eigenvalues of the P2006T.

According to the results observed in Figure 4 all the modes are stable. However, a more exhaustive study varying different conditions, such as altitude, velocity, and weight and C.G. position, has shown that in some of those conditions the P2006T has an unstable spiral mode.

To conclude with the aerodynamic data, Figure 5 depicts the drag polar of the complete aircraft calculated by different methods: Torenbeek [9], Digital DATCOM and the parabolic approximation of the drag polar evaluated by Torenbeek's method [9]. The relative error of the parabolic approximation is about 10% lower than the real drag polar.

At this point, all data related to the aerodynamic model are validated. Now it is time to deal with the propulsive model.

First it is necessary to know some parameters of the P2006T real engine, a Rotax 912 S3, in order to estimate its operating curves. Once this has been solved, the required power and the available power in the propeller are needed in different flight conditions.

If we compare the operating curves calculated with the Rotax manual curves [10] a relative error is observed that is around 5-15% lower than the real power, depending on the operating point selected.

The required power for cruise flight is defined as the dissipated power multiplied by the aerodynamic drag. If the flight condition is a climb or a descent, then the weight of the aircraft needs to be taken into account. The power is usually expressed in terms of the equivalent speed and using the drag polar of the complete aircraft. Also, it will be assumed that the angle of climb or descent is very small. According to this, the corresponding equations to calculate the required power in the three different previous conditions are the following:

$$P_d\sqrt{\sigma} = \frac{1}{2}\rho_0 V_{EAS}^3 S_W \left(A + B\frac{W}{\frac{1}{2}\rho_0 V_{EAS}^2 S_W} + D\left(\frac{W}{\frac{1}{2}\rho_0 V_{EAS}^2 S_W}\right)^2 \right) \quad (23)$$

$$P_{req.\,climb} = W V_{EAS}\gamma + \\ + \frac{1}{2}\rho_0 V_{EAS}^2 S_W \left(A + B\frac{W}{\frac{1}{2}\rho_0 V_{EAS}^2 S_W} + D\left(\frac{W}{\frac{1}{2}\rho_0 V_{EAS}^2 S_W}\right)^2 \right) \quad (24)$$

$$P_{req.\,descent} = -W V_{EAS}\gamma + \\ + \frac{1}{2}\rho_0 V_{EAS}^2 S_W \left(A + B\frac{W}{\frac{1}{2}\rho_0 V_{EAS}^2 S_W} + D\left(\frac{W}{\frac{1}{2}\rho_0 V_{EAS}^2 S_W}\right)^2 \right) \quad (25)$$

Finally, the equation that allows calculating the power in the propeller is the following [6]:

$$P_u = (P_m N_e - P_{mechanical} - P_{electrical})\eta_{gear}\eta_p \quad (26)$$

Where 'Pm' is the corresponding power to the operating point of the engine, 'Ne' is the number of engines, 'Pmechanical' and 'Pelectrical' is the power demanded by the mechanical and electrical systems of the aircraft respectively, 'ηgear' is the efficiency of the reduction gear and 'ηp' is the propeller efficiency. All these coefficients, except the latter, can be estimated by Roskam [6].

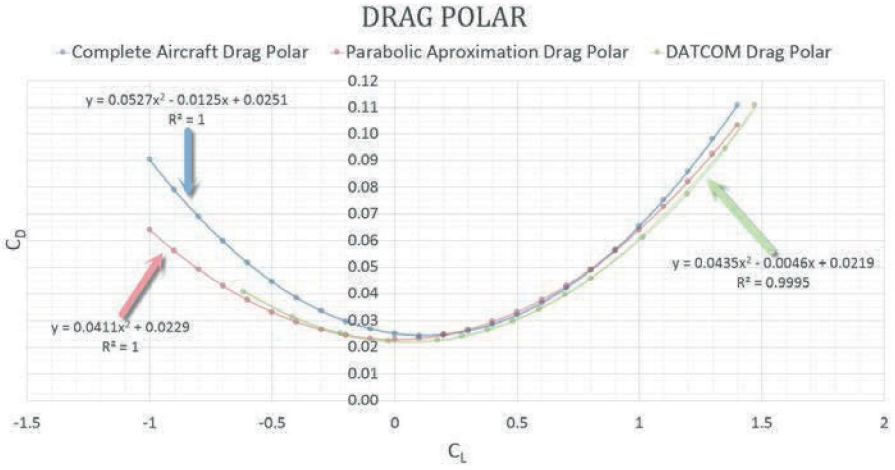

Fig. 5. Different drag polar representations.

Additionally, a method developed by the NACA (National Advisory Committee for Aeronautics) [11] has been used to calculate the propeller efficiency, based on the variable-pitch and constant speed propeller equipped in the P2006T. This method shows good behaviour for cruise conditions, and for flight conditions near to stall NACA recommends using experimental data of the real engine-propeller combination.

The curves associated with the required and the available power at cruise conditions are represented in Figure 6.

It is now possible to build the simulator in Simulink using all of the previous results. After that, some tests will be evaluated to check the behaviour of the simulated P2006T, comparing the results with the features and behaviour of the actual aircraft, described in part II of this paper.

One of the tests consisted in letting the aircraft fly without varying the controls to confirm the aerodynamic model through the short period, phugoid, spiral, roll and Dutch roll dynamic response. The test to validate the propulsive model is done by introducing the aircraft under a specific flight condition defined by an altitude and an operating point of the engine to verify the speed achieved. Another way of testing the propulsive model is by operating the engine at maximum revolutions at a certain initial altitude and checking the absolute ceiling reached.

The last test required is the integral performance of the P2006T to evaluate the specific fuel consumption and the effective power provided by the engine. This test is done by checking the range and endurance throughout the design mission.

Below are the different graphs showing selected results extracted from simulator outputs. In most cases the relative error in comparison with the real aircraft is lower than 10%.

Figure 7 represents different time evolutions of the theta body angle, body speed and angle of attack. Through these curves the phugoid mode can be seen. During the first seconds of these graphs, the short period mode can be seen. In the same way that phugoid, the short period and the lateral-directional modes (roll, spiral and Dutch roll) can be represented.

Figure 8 represents the altitude and the body speed to check the absolute ceiling reached. The relative error in this case is 0.6% in altitude and 7.5% in speed, in relation to the values of the real P2006T platform [12].

Figure 9 represents the power demanded when the aircraft is flying at a fixed cruise speed of 250 kilometres/hour and at an altitude of 2134 meters, both variables imposed in the autopilot. The relative error achieved is 3.8% with respect to the effective power of the real P2006T [12].

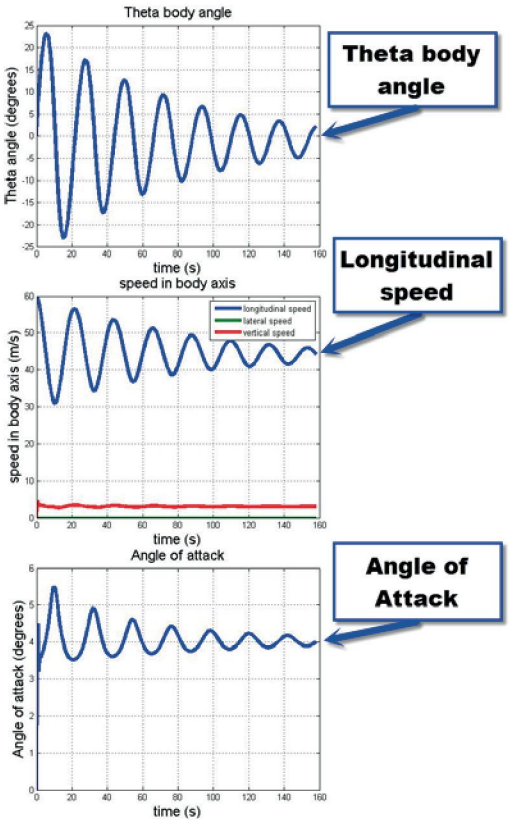

Fig. 7. Phugoid of the P2006T. The main variables are the theta body angle, longitudinal speed and angle of attack.

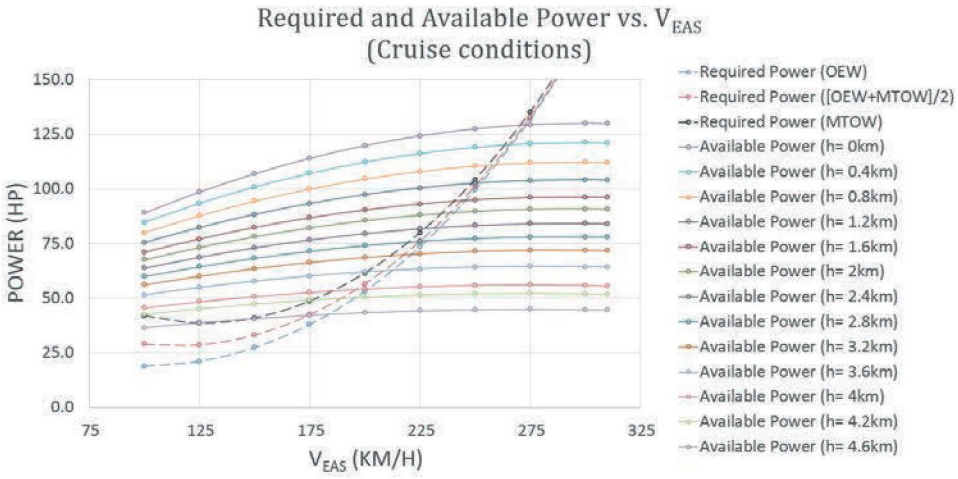

Fig. 6. Required power vs. available power of P2006T.

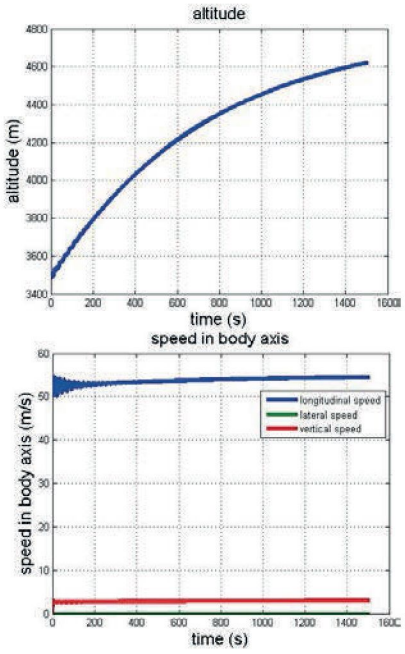

Fig. 8. Ceiling simulation. Above the altitude, below, in blue, the longitudinal speed.

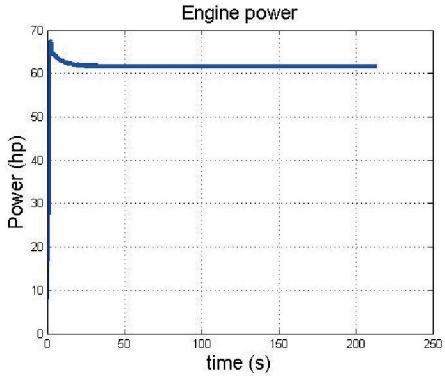

Fig. 9. Power demanded (hp) at 250 km/h and 2134 m.

Finally, the relative error achieved in the test to verify the integral performances is about 8.9%, in relation to the real P2006T [12].

The previous results are used to demonstrate the accuracy of the simulator developed in this work. Then, from this moment, the Rotax 912 S3 engine will be replaced by the electric motor based on axial flux technology. Also, the design mission will be implemented in the autopilot to view the consumption achieved and to design the required batteries. In addition, it is advisable to calculate the necessary hinge moments in the surface controls in order to develop new actuators if necessary. In the next part of this paper the output data obtained with the axial flux electric motor will be described.

TABLE I. DIFFERENT TEST TO CHECK THE PRECISION OF THE SIMULATOR.

	Obtained value	*Expected value*	*Relative error*
Ceiling	4600 m	4572 m	0.6%
Power at 7000ft. And 250km/h	62 hp	64.5 hp	3.8%
Power at maximum speed at Sea Level	87.5 hp	92.5 hp	5.4%
Maximum speed at Sea Level	277 km/h	287 km/h	3.5%
Stall speed	99 km/h	104 km/h	4.8%
Range (65% power, 30 minute reserves)	1045 km	1148 km	8.9%
Endurance (65% power, 30 minute reserves)	4.68 h	4.65 h	0.64%

TABLE II. CLIMB TESTS TO CHECK THE PRECISION OF THE SIMULATOR.

	V (m/s)			P (hp)		
h (m)	*Obtained value*	*Expected value*	*Relative error*	*Obtained value*	*Expected value*	*Relative error*
800	57	54.86	3.75%	80	84.5	5.63%
1600	54	50	7.41%	72	77.78	8.03%
2400	50	45.34	9.32%	65	68.39	5.22%
3200	46	39.1	15.00%	59	61.7	4.58%

IV. BUILDING THE FINAL SIMULATOR.

In the last version of the simulator, it was necessary to change the Rotax engine of the real P2006T platform for the AF-130. This engine is manufactured by EVO Electric and its operating curves are shown in Figure 10.

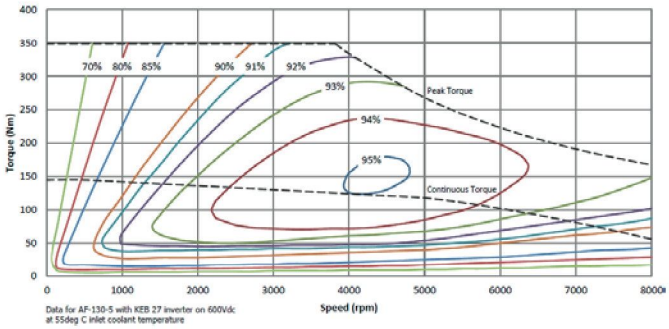

Fig. 10. Operating curves of axial flux electric motor. [18]

The performances of the P2006T with this new engine are different. The AF-130 provides less power than the Rotax 912 S3 at sea level. However, the power of the electric motor does not change with the altitude of flight as occurs with the Rotax.

This behaviour of the engine enables the aircraft to fly at higher altitudes. The greater the altitude the lower the aerodynamic drag, because the density is lower than its value at sea level. So the aircraft can fly faster at a higher altitude, reaching a higher cruise speed. In conclusion, the ceiling of the P2006T with the electric motor is limited by its never exceed speed (VNE) of 311 kilometres/hour.

The graphs with the performances of P2006T with the AF-130 electric motor are shown below. Figure 11 represents the ceiling of the P2006T, established at 10650 metres. Figure 12 represents the maximum cruise speed at sea level. Note that the speed at sea level is lower than the speed at ceiling, as was stated previously. In both tests, the engine was operating at constant revolutions, set at 4200 RPM, and the level of power supplied vertically varied in the operating curves of Figure 10.

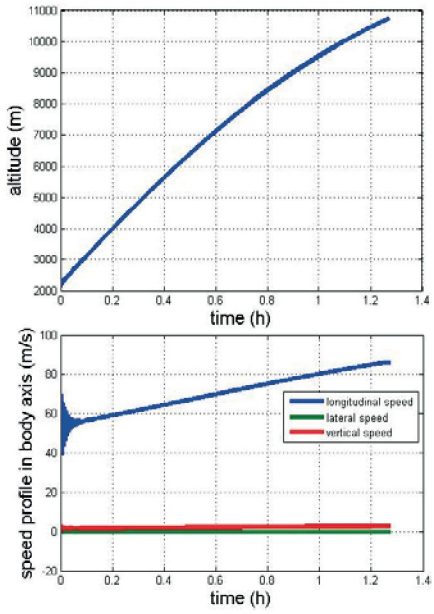

Fig. 11. Ceiling of the P2006T with the electric motor. Above the altitude, below, in blue, the longitudinal speed.

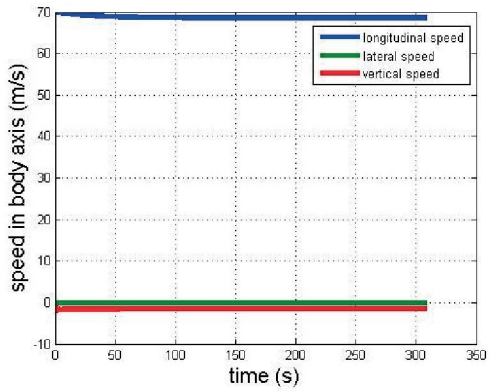

Fig. 12. Maximum cruise speed (in blue) at sea level at 4200 RPM.

The last test consisted in carrying out the design mission according to the altitude profile of Figure 1, also specifying the speed of each segment of the mission. Figure 13 is the power demanded and Figure 14 is the hinge moment of the all-moving tailplane of the P2006T to ensure the flight altitude in the autopilot.

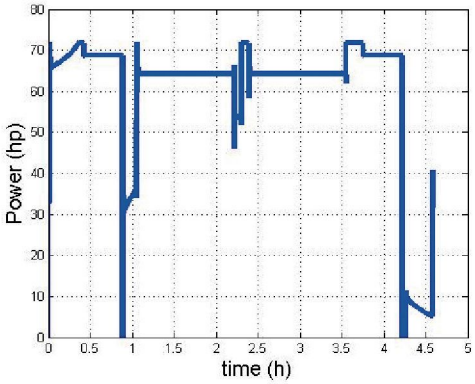

Fig. 13. Demanded power profile of the simulated design mission.

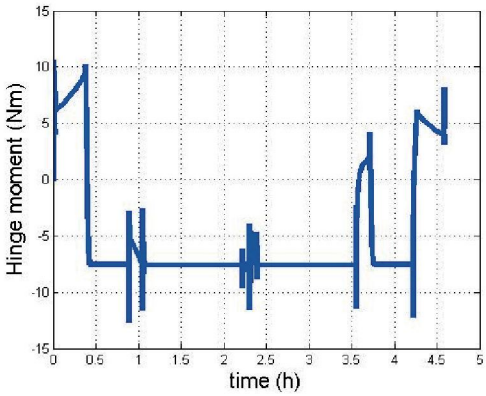

Fig. 14. Hinge moment of the all-moving tailplane of the simulated design mission.

The total consumption throughout the complete design mission with a battery efficiency of 100% was 390 kilowatt-hours. The weight of the required batteries to accomplish the mission would be around 2925 kilograms. This weight is excessive because the P2006T can equip a maximum weight of batteries of 576 kilograms without a pilot in unmanned mode. This consumption makes the full electric aircraft not valid for the defined mission, it probably being necessary to restrict the application of this full electric version only to specific short range missions or consider some kind of hybridization. So, it will be necessary to think of some way of hybridization in order to increase the time that the aircraft is able to fly with the electric powertrain based on the defined electric motor. Several options can be considered, ranging from high power density rotary engines coupled to a generator to fuel cell implementation. Sizing these hybridization alternatives can be carried out using the simulation tool described in this paper.

V. Conclusions

The calculation of the performances and the behaviour of the model developed for P2006T seems to be accurate compared with the data provided by the manufacturer [12], [13] and other data from a study carried out by the Federico II University of Naples with the real aircraft [14].

In accordance with all the statements in the previous paragraphs, the relative error of the results observed in the

output data of the initial simulator tests are lower than the limit of the usual 10% relative error in preliminary designs. This has allowed making some tests with other kinds of engine and beginning to develop new possible types of electric and hybrid propulsion. In addition, one module has been implemented in order to estimate the hinge moment of the controls in every flight condition for evaluating the requirements of the actuators that may govern these control devices. The simulation tool has been used to evaluate the requirements in terms of energy for a full electric powered aircraft, providing an estimation of battery size or achievable range considering the limitations to aircraft payload.

The hinge moment is considered of interest in order to evaluate the forces of hydraulic actuators, due to the fact that these elements can be changed in the future to electrically operated actuators, enabled by the presence of a significant electric power supply coming from the energy storage system.

It is important to highlight that the simulation model developed will be executed in real time platforms when this platforms are built, so that components related to the propulsion system and actuators can follow a "model-based" development approach, which will be of great value for applied research in this novel field of hybrid /electric propulsion and electro-mechanic actuation.

In order to estimate the performance of the new designed components, different modules should be taken into account such as wind models, avionics or navigation systems as well as new codes, etc. Despite this amount of work, developing these types of tools in the design process of new systems is highly interesting and enables both cost and developing time to be reduced.

ACKNOWLEDGMENTS

This work has been supported by the Tecnalia Research & Innovation project Ref. P130135160.

REFERENCES

[1] National Aeronautics and Space Administration (NASA), "Green Aviation : A Better Way to Treat the Planet." NASA Facts, Washington, pp. 1–2, 2013.

[2] J. Valera, I. Iglesias, and A. Peña, "Integrated Modeling Approach for Highly electrified HEV. Virtual Design and Simulation Methodology for Advanced Powertrain Prototyping.," pp. 1–8, 2009.

[3] A. Pena, I. Iglesias, J. Valera, and A. Martin, "Development and validation of Dynacar RT software, a new integrated solution for design of electric and hybrid vehicles," dynacar.es, pp. 1–7, 2012.

[4] INDRA, "P2006T MRI SURVEILLANCE SYSTEM," 2011.

[5] The USAF Stability and Control Digital DATCOM Volume I , Users Manual, First., vol. I. Niehaus, B. F.; Hoehne, V. O.; Ostgaar, Morris A., 1979.

[6] J. Roskam, Airplane Design: Part 6, First edit. Lawrence, Kansas, 1987.

[7] J. Roskam, Methods For Estimating Stability And Control Derivatives Of Conventional Subsonic Airplanes, Second edi. Lawrence, Kansas, 1973.

[8] C. Gómez Tierno, M. Á.; Pérez Cortés, M.; Puentes Márquez, Mecánica del vuelo, Segunda ed. Madrid: IBERGARCETA PUBLICACIONES, 2012, pp. 1–482.

[9] E. Torenbeek, Synthesis of subsonic airplane design. Delft, 1976.

[10] ROTAX, Manual del Usuario ROTAX 912, First edit. 1998.

[11] National Advisory Committee for Aeronautics (NACA), "Propeller-efficiency charts for light airplanes," Washington, 1947.

[12] P. Jackson, Ed., Jane's All the world's Aircrafts 2013-2014, 100th edit. Jane´s Information Group.

[13] TECNAM, Tecnam p2006t, Aircraft flight manual, Second., vol. 39, no. 2006. Capua: TECNAM, 2010.

[14] F. Nicolosi, A. De Marco, and P. Della Vecchia, "The Role of Flight Tests and of Flight Simulation in Aircraft Design," Naples, 2011.

[15] INDRA, "Search capability of the tecnam mri surveillance system," 2011.

[16] R. G. Driggers, M. Spie, and M. Kelley, "National imagery interpretation rating system and the probabilities of detection , recognition , and identification," Opt. Eng., vol. 36, no. 7, 1997.

[17] R. Austin, Unmanned Aircraft Systems. Chichester, UK: John Wiley & Sons, Ltd, 2010.

[18] EVO Electric Ltd., "AF-130 Motor | Generator AF-130 Specification Performance and Efficiency (Motor Operation)," vol. 44, no. 0. EVO Electric Ltd., pp. 1–2, 2011.